Spatially-guided non-local mean filter for denoising of clinical whole-body PET images

Hossein Arabi and Habib Zaidi†, *IEEE Fellow*

***Abstract*– A novel spatially-guided non-local mean (SG-NLM) filter for denoising whole-body PET images is proposed. In this approach, PET images are first clustered into a number of regions with homogeneous uptake and a Bayesian framework exploited to estimate the noise level for automatic parameter setting. Then, instead of defining a search window to find similar patches (as in conventional NLM), only patches belonging to the same regions are collected and compared to facilitate the patch searching process. The SG-NLM filter was compared to conventional post-reconstruction Gaussian and NLM filters. Experimental measurements using the Jaszczak phantom and clinical whole-body PET/CT studies were used to evaluate the performance of the proposed approach. In the Jaszczak phantom, the signal to noise ratio (SNR) improved from 26.5 when using Gaussian smoothing to 29.9 and 30.7 (averaged over all six spheres in the Jaszczak phantom) using the NLM and SG-NLM filters, respectively. The clinical studies further demonstrated the superior performance of SG-NLM method by leading to higher SNR while yielding a quantification change in malignant lesions of -2.4% compared to -11.7% and -2.9% achieved using Gaussian and conventional NLM filters, respectively. The SG-NLM proved to improve the contrast, SNR and quantitative accuracy compared to Gaussian and NLM approaches, and can be utilized as an alternative post-reconstruction filter in clinical whole-body PET/CT imaging.**

I. Introduction

PET commonly suffers from high noise level, particularly in protocols with very short acquisition times or low-dosages (e.g. paediatric PET protocols), and dynamic studies. A potential solution is to use edge-preserving filters, such as non-local mean (NLM), which are capable of suppressing noise while preserving prominent signals [1]. The NLM denoising was reported to outperform other edge preserving approaches, particularly for white Gaussian noise [2]. A novel NLM denoising approach is proposed for enhancing the quality of whole-body PET studies. In the conventional NLM filter, a search window is defined to limit the exhaustive search for finding similar patches of voxel to reduce the computation burden; otherwise the entire image should be explored that is computationally expensive particularly for 3D images [3]. However, a lot of useful information residing out of the search window is neglected. We propose a spatially-guided NLM (SG-NLM) approach which does not entail the search window and at the same time does not impose additional computation burden. This approach benefits from noise variance estimation for automatic tuning of smoothing parameters. To this end, the PET image is clustered into a number of regions with homogeneous uptake, and then a Bayesian maximum a posteriori probability (MAP) framework is exploited to estimate an upper bound of the real noise level function by fitting a lower envelope to the standard deviations of each segment. The obtained noise level estimation is used for automatic adjustment of SG-NLM smoothing parameters. In the SG-NLM approach, there is no search window and the search for finding similar patches is only conducted on the same regions. For instance, if the target voxel to be filtered belongs to cluster or region #N (Fig. 1 II.SG-NLM B), the search for finding similar patches is only carried out on region #N, which can be extended through the entire image, thus dramatically increasing the chances to find proper similar patches. In addition to homogeneous regions, an extra class is defined for the prominent edges (Fig. 1 II.SG-NLM C). If the target voxel is located on an edge, the patch search is only carried out on the voxel belonging to this cluster (prominent edges). The SG-NLM explores the entire image for spotting similar patches which enhances the performance of NLM filtering without adding significant additional computational burden.

II. Materials and Methods

A. Noise variance estimation

The upper bound of the noise intensity was estimated from the noisy image without any prior knowledge about the noise level using the method described in [4]. The noise variance estimation is carried out based on a piecewise smooth version of the noisy image. Given the piecewise smooth image, a Bayesian MAP framework is exploited to establish a correlation between noise level and the signal intensity. The noisy image voxels are grouped into piecewise homogeneous regions according to intensity similarity and spatial connectivity using a K-means clustering algorithm [5]. Image clustering generates patches of voxels represented by mean intensity and variance. The estimation of the noise variance is performed through fitting a function to all sample points of the variance.

B. Non-local mean filter (NLM)

NLM filters take advantage of the existing redundant information (repeated patterns) in natural images for noise suppression. In NLM filters, patches of images representing similar patterns are selected and averaged to preserve the underlying pattern and eliminate the noise component. The averaging

H. Arabi is with the Division of Nuclear Medicine & Molecular Imaging, Geneva University Hospital, CH-1211, Geneva, Switzerland (e-mail: hossein.arabi@unige.ch).

†H. Zaidi is with the Division of Nuclear Medicine and Molecular Imaging, Geneva University Hospital, CH-1211 Geneva, Switzerland, Geneva University Neurocenter, CH-1205 Geneva, Switzerland. He is also with the Department of Nuclear Medicine and Molecular Imaging, University of Groningen, University Medical Center Groningen, Groningen, Netherlands, and the Department of Nuclear Medicine, University of Southern Denmark, DK-500, Odense, Denmark (e-mail: habib.zaidi@hcuge.ch).

978-1-5386-8494-8/18/$31.00 ©2018 IEEE

process is weighted based on similarity between the patch of the image centered at the target voxel and a number of non-local patches. The search for finding similar patches plays a determining role in the performance of NLM filters, which is normally conducted within a predefined spatial constraint, called the search window. This search window is normally defined as a fixed sub-dimension of the image to limit the search space where exhaustive search throughout the image may be computationally expensive [6].

C. Spatially-guided non-local mean filter (SG-NLM)

The clustered image obtained from noise variance estimation is used to guide the NLM filter to conduct a far more effective search for finding similar patches. In the SG-NLM filter, there is no search window and instead, the search for similar patches is conducted in regions having the same uptake. To this end, the regions in the clustered image obtained from the previous section are labelled (1 to N) according to their intensity level. Give the label of the target voxel to be filtered (for instance N); the search for finding similar patches is only carry out in the regions with the same labels. In the conventional NLM (Fig. 1 I.NLM), the search window (green) is first centred on the target voxel, then all possible patches (I.NLM A) are examined to give greater weights to more similar patches (I.NLM B). However, in the SG-NLM, the search for similar patches is only carry out in regions with the same uptake or label, which is not limited locally and can be extended within the whole 3D image (II.SG-NLM B). Moreover, an extra label is dedicated to the prominent edges obtained from the Sobel edge detector (II.SG-NLM C). If the target voxel resides on the edge label, the search for similar patches is only conducted on the edge label. This search scheme guarantees more efficient patch searching (II.SG-NLM D) without significant additional computational burden.

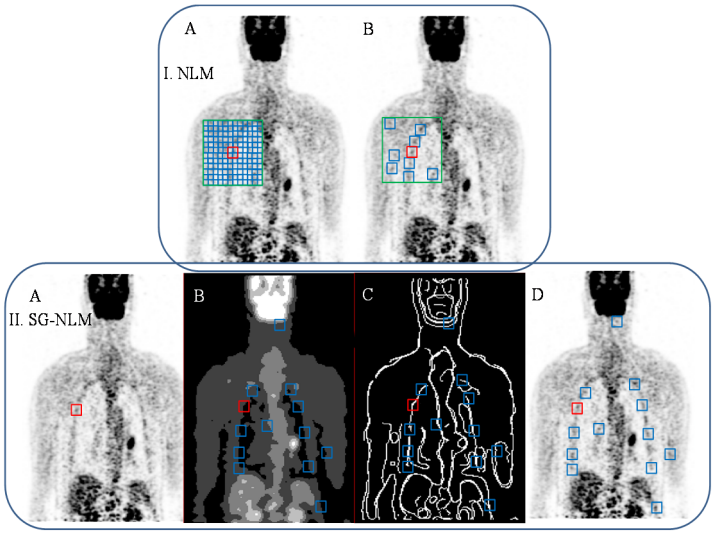

Fig 1. I.NLM: A) Conventional NLM search window, B) similar patches. II:SG-NLM: A) Target patch, B) clustered image, C) additional edge label, D) similar patches.

D. Evaluation strategy

The proposed SG-NLM filter was compared with conventional NLM and Gaussian filters. The physical Jaszczak phantom with an activity concentration ratio of 5:1 between hot spheres and background was scanned on the mCT PET/CT scanner. The list-mode data were then reconstructed for durations of 30 min, 10 min, 3 min, 1 min, 30 sec, and 10 sec to realize different noise levels. In addition, 35 VOIs were defined on malignant lesions of 12 clinical whole-body PET/CT studies to compare the noise level in the target and background volumes before and after filtering. The performance of the different approaches was quantitatively evaluated using the contrast-to-noise ratio (CNR) (Eq. 1), Bias (%) (Eq. 2) as well as SNR (Eq. 3) for different VOIs.

$$CNR = \frac{|\mu_{signal} - \mu_{background}|}{\sqrt{\frac{|\sigma^2_{signal} + \sigma^2_{bakcground}|}{2}}} \quad (1)$$

$$Bias(\%) = \frac{100}{Lr}\sum_{i=1}^{Lr}\frac{|(\mu_{signal_i} - Tl)|}{Tl} \quad (2)$$

$$SNR = \frac{\frac{1}{Lr}\sum_{i=1}^{Lr}(\mu_{(signal)i} - \mu_{(background)i})}{\frac{1}{Bg}\sum_{j=1}^{Bg}\sigma_j} \quad (3)$$

μ_{signal} and $\mu_{background}$ denote the mean values of the target and background VOIs in the filtered images and σ^2_{signal} and $\sigma^2_{bakcground}$ the corresponding standard deviations, respectively. Tl is the true intensity value within the phantom VOIs and Lr is the number of different noise realizations. Bg denotes the total number of voxels within the background VOI and σ_j is the ensemble standard deviation of each voxel j across the noise realizations. For the clinical studies, the changes after applying the different denoising algorithms were computed using Eq. (4) considering the original noisy image as baseline.

$$Change(\%) = \frac{\mu ROI_{filtered} - \mu ROI_{noisy}}{\mu ROI_{noisy}} \times 100\% \quad (4)$$

III. Results and Discussion

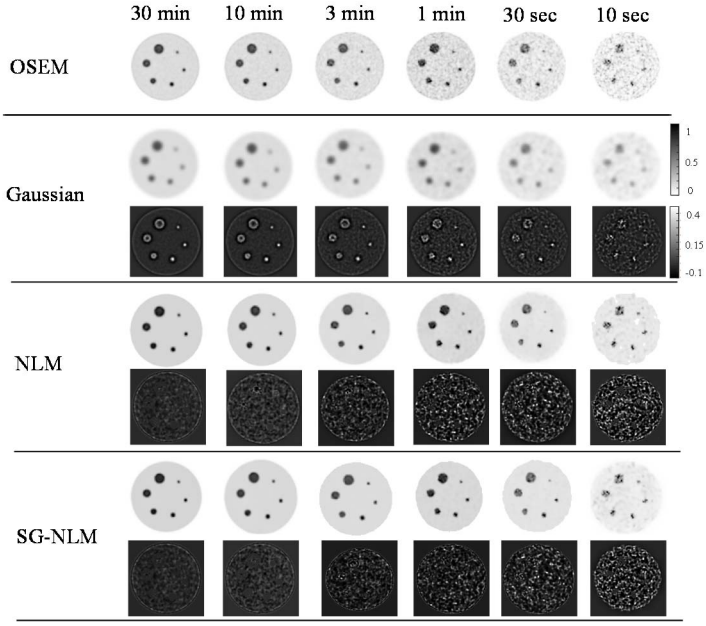

Fig 2. OSEM reconstructions and filtered images of the experimental Jaszczak phantom with different acquisition times along with corresponding residual images.

The results of the experimental Jaszczak phantom filtered by the different approaches are illustrated in Fig. 2. Considerable resolution and signal recovery can be observed in the images filtered using the SG-NLM approach. The Gaussian filter led to important loss of contrast and signal particularly for the small spheres while NLM and SG-NLM filtering exhibited superior performance for images with low SNR.

SG-NLM led to lower bias and improved CNR across the spheres with a maximum bias of 31.8% compared to 35.4% and 32.0% for Gaussian and NLM filters, respectively (Table 1). The maximum CNR (24.7) was obtained using the SG-NLM approach for the largest sphere, whereas Gaussian filtering yielded minimum CNR (6.3) for the smallest sphere.

Table 1. CNR, SNR and quantification bias measured in the different spheres of the Jaszczak phantom before and after filtering.

Spheres		OSEM	Gaussian	NLM	SG-NLM
1	Bias(%)	29.2	35.4	32.0	31.8
	SNR	20.2	25.1	27.9	28.4
	CNR	5.9	6.3	12.9	13.2
2	Bias(%)	27.4	32.6	30.9	30.5
	SNR	21.0	25.9	28.3	29.6
	CNR	6.2	8.4	13.1	13.3
3	Bias(%)	25.2	30.7	28.1	28.7
	SNR	21.7	26.4	29.1	29.8
	CNR	8.2	11.3	17.8	18.4
4	Bias(%)	25.1	28.5	27.2	27.1
	SNR	22.6	26.9	31.3	32.0
	CNR	9.1	14.3	21.6	21.9
5	Bias(%)	24.3	27.0	25.9	25.8
	SNR	23.0	27.3	31.4	32.1
	CNR	8.2	14.1	22.1	22.2
6	Bias(%)	22.3	24.7	23.9	23.9
	SNR	22.8	27.2	31.5	32.2
	CNR	9.1	13.5	24.1	24.7

Qualitatively, the clinical images were efficiently denoised whatever the method used. However, SG-NLM showed the lowest change in terms of quantification (%) for malignant lesions while resulting in highest (30.9) SNR (Table 2).

Table 2. CNR, SNR, average lesion and lung activity concentrations, and quantification bias measured on VOIs defined on lesions.

	OSEM	Gaussian	NLM	SG-NLM
CNR	12.1	14.2	22.0	22.7
SNR	22.4	25.6	30.3	30.9
Average lesion activity concentration (SUV) (Standard deviation)	7.3 (1.4)	6.4 (1.0)	7.0 (0.6)	7.1 (0.6)
Average lung activity concentration (SUV) (Standard deviation)	0.28 (0.096)	0.21 (0.063)	0.24 (0.048)	0.25 (0.046)
change (%)	-	-11.7	-2.7	-2.4

IV. Conclusions

A novel NLM denoising approach for PET images was developed enabling to enhance the performance of the conventional NLM filter through conducting an efficient patch search. Experimental and clinical PET studies demonstrated that the proposed approach outperformed conventional Gaussian and NLM denoising techniques. The SG-NLM denoising approach could replace conventional Gaussian filtering since it provides superior noise reduction and signal preservation.

Acknowledgements

This work was supported by the Swiss National Science Foundation under grant SNSF 320030_176052 and the Swiss Cancer Research Foundation under Grant KFS-3855-02-2016.

References

[1] H. Arabi and H. Zaidi, "Improvement of image quality in PET using post-reconstruction hybrid spatial-frequency domain filtering," *Phys Med Biol,* vol. 63(21), p. 215010(17), 2018.

[2] C. Chan, R. Fulton, R. Barnett, D. D. Feng, and S. Meikle, "Postreconstruction nonlocal means filtering of whole-body PET with an anatomical prior," *IEEE Trans Med Imaging,* vol. 33(3), pp. 636-650, 2014.

[3] A. Buades, B. Coll, and J.-M. Morel, "A non-local algorithm for image denoising," in *2005 IEEE Computer Society Conference on Computer Vision and Pattern Recognition (CVPR'05)*, pp. 60-65, 2005.

[4] C. Liu, W. T. Freeman, R. Szeliski, and S. B. Kang, "Noise estimation from a single image," *IEEE Computer Society Conference on Computer Vision and Pattern Recognition, 2006*, pp. 901-908, 2006.

[5] C. Zitnick, N. Jojic, and S. B. Kang, "Consistent segmentation for optical flow estimation," *Tenth IEEE International Conference on Computer Vision, ICCV2005*, pp. 1308-1315, 2005.

[6] Z. Xu, M. Gao, G. Z. Papadakis, B. Luna, S. Jain, D. J. Mollura*, et al.*, "Joint solution for PET image segmentation, denoising, and partial volume correction," *Med Image Anal,* vol. 46, pp. 229-243, 2018.